Proceedings of the IASS 2024 Symposium
Redefining the Art of Structural Design
August 26-30, 2024, Zurich Switzerland
Philippe Block, Giulia Boller, Catherine DeWolf,
Jacqueline Pauli, Walter Kaufmann (eds.)

An early design stage parametric exploration of integrated concrete funicular floor element and thermal mass performance for carbon footprint reduction

Zherui WANG*[a], Hua CHAI[a], Xiaoxiao PENG, Ryan WELCH[b], Masoud AKBARZADEH[a], Dorit AVIV

*Thermal Architecture Lab, Weitzman School of Design, University of Pennsylvania, Philadelphia, USA
zheruiw@upenn.edu

[a] Polyhedral Structures Laboratory, Weitzman School of Design, University of Pennsylvania, Philadelphia, USA
[b] KieranTimberlake, 841 N American St, Philadelphia, PA, USA

Abstract

In response to the imperative of reducing material use and carbon footprint, building structural elements can be designed with structural and environmental design considerations for duo-functions. We present an early-stage, parametric design workflow that integrates thermal mass performance with structurally optimized, prefabricated, funicular, concrete floor elements. Thermally massive building structures, like concrete floors, can act as a thermal battery that reduces reliance on and carbon emission associated with mechanical cooling. The proposed co-design workflow forges an integrated structural and building energy simulation framework that assesses the operational carbon saving associated with cooling induced by different building structural thermal mass design options, while constraining the embodied carbon associated with material volume. Polyhedral Graphic Statics (PGS) is utilized as the geometric form-finding method to intuitively design and optimize the discrete floor geometry via Polyframe, a parametric plugin developed in Grasshopper. The floor geometries are then placed in the whole building energy simulation environment to evaluate its thermal mass performance impact on lifecycle carbon emission reduction related to space cooling with Future Typical Meteorological Year (fTMY) weather data. Projected hourly average grid emission factors from 2020 to 2079 are referenced for emission calculations. Using the US Department of Energy Secondary School Reference Building as a case study, the 60 year life cycle cooling carbon emission savings associated with structurally optimized thermal mass floors are investigated in two representative cities in two climate zones and grid emission scenarios (marine climate in San Diego, California, and cold climate in Denver, Colorado). Our results reveal that using co-designed concrete funicular floors as building thermal mass can achieve 25% and 15% annual cooling carbon emission reduction compared to the flat slab of the same material volume in San Diego and Denver respectively from 2020 to 2039. With further grid electrification, a 9% and 10% reduction can be obtained from 2040 to 2059, and 0 and 6% from 2060 to 2079 in the respective locations.

Keywords: Form-finding, polyhedral graphic statics, multi-criteria design, structural thermal mass, carbon reduction

1. Introduction

According to the 2019 International Energy Agency reports, buildings are responsible for over 39% of combined embodied and operational carbon emission globally [1]. To confront the escalating carbon emission associated with building construction and operation, building floor elements can be designed with both structural and environmental considerations when multiple-functionality is possible.

Structurally efficient floor elements allow materials saving, and by extension reduced embodied carbon emissions, which contributes to 11% of global carbon emissions [1]. Environmental performance analysis aims to minimize building operational energy and operational carbon emissions, which accounts for 28% of global direct-use emissions [1]. With the changing climate, the carbon emission related to space cooling alone is responsible for 7% of global greenhouse gas emissions, and is expected to triple by 2050 as temperatures continue to rise [2]. In this context, designing building floor elements that can reduce both embodied and operational carbon emissions, particularly operational emission related to cooling, becomes crucial.

While concrete structures can be carbon intensive, funicular floor elements bear the integrative potential in curbing both embodied and operational carbon emissions in comparison to conventional flat slabs. The funicular load paths of the floor are optimized for minimum material weight, and by extension the embodied carbon associated with material use. At the same time, the thermally massive property of concrete allows the funicular floor elements to function as thermal mass. When coupled with natural ventilation, building thermal mass (BTM) can reduce operational energy associated with mechanical cooling, and by extension operational carbon.

The basic principle of BTM is that the storage material absorbs and stores heat during the day and releases it at night, with the aid of natural ventilation. In this manner, BTM provides indoor temperature damping and shift, and alleviates over-reliance on mechanical cooling. However, BTM is not always advantageous and can result in escalated operational energy consumption when its amount is not properly calibrated to the climate conditions and building characteristics [3]. The effectiveness of thermal mass is co-determined by the functioning of transient heat conduction and storage, surface convection, and sufficient airflow. These four co-determining key factors can be synchronized with natural ventilation for desired response time and thermal mass performance [4]. This demands BTM to be designed for their surface area, mass thickness, overall material volume based on the thermal property.

The use of Polyhedral Graphic Statics (PGS) bears utility in achieving this goal, given its versatility in generating structurally considered design and thermal mass distribution simultaneously. With the same constraints on the loading scenario and structural footprint, different structural forms with varying surface area and member thickness can be designed by manipulating the form-force reciprocal diagram, while the corresponding material volume required to resist applied loads are maintained. This enables the integrative and simultaneous exploration of structural form-finding and thermal mass performance early in the design process.

We propose an early stage, parametric co-design workflow that considers structural form-finding and thermal mass performance using operational carbon emission associated with cooling as the assessment metric. This workflow enables the generation of various funicular floor design options to be assessed while adhering to constraints on material volume and corresponding embodied carbon. While the performance of using building structure as thermal mass and its lifecycle embodied and operational carbon impact have been assessed [5], [6], their integrated, early stage, co-design consideration has not been thoroughly explored, particularly for funicular elements designed with PGS.

Furthermore, with the advent of advanced manufacturing, techniques like robotic 3-D printing allows concrete funicular floor elements, with varying geometric features and surface area exposure constrained by material volume, to be fabricated with increasing ease in full-scale [7]. Simultaneously, recent study shows that expanding BTM surface area by a factor of 1.7, under a material volume constraint, can improve indoor temperature damping and annual occupant thermal comfort by 6% and 7% in hot-dry and marine climates, respectively, leading to operational energy and carbon emission savings [8]. This context provides the broader applicability and necessity in embedding both structural design and thermal mass performance in the early stage design workflows, and evaluating their combined performance and contribution to carbon emission.

2. Methods

This section outlines the workflow first on the structural form-finding with PGS considering the thermal mass performance of the funicular floor design; second the incorporation of design options in the whole building energy simulation to obtain annual operational energy use results; and finally the operational carbon emission assessment on cooling related to different floor design options.

2.1. Parametric Co-design Workflow

2.1.1. Structure design with 3-dimensional polyhedral graphic statics

The geometry of the floor element is generated computationally using Polyframe [9], a Grasshopper plug-in, based on the algebraic polyhedral graphic statics form-finding process [10]. The method defines the floor's initial model based on the boundary condition and loading scenarios. We reference the footprint of a room detailed in Section 2.2.1 of the case study, where the dimensions are 11m by 9m (length by width). The applied load consists of a live load and a self weight component. The live load is assumed to be 2.5kN/m^2, while the self-weight is assumed to be 25% of the total live load. We acknowledge that this simplified design criteria may not correspond to the final structure weight of the design option generated, and may require an iterative process for their alignment. This will be addressed in future work. By establishing the algebraic edge constraints, different structural floor concepts can be generated by manipulating the locations and directions of the vertices and edges and subdividing the faces of the form-force reciprocal diagrams. This technique allows the generation of funicular forms under different load paths and force magnitudes, resulting in different surface areas and material thicknesses required to resist principal axial stresses. Figure 1 shows three options of the form and force reciprocal diagrams under the same loading and boundary conditions. Design option 1 and 2 are tension-compression combined systems with a concave downward-facing ceiling surface. Design option 3 is a compression-only system where the downward-facing ceiling surface is convex and vaulted.

Next, the top and internal faces of the form diagram are materialized with concrete. Each face is assigned a thickness based on the principle axial stress, which is calculated based on the compressive strength of the concrete (25MPa) and the magnitude of forces derived from the faces of the form and force reciprocal diagrams. Figure 2 shows the three design options materialized with different topping and rib thickness, and surface area exposure, constrained by the same material volume.

It is acknowledged that the structural form-finding process is targeted for early design stage study, and provides benefit in designing material distribution under structural design considerations that also have implications for thermal mass performance (detailed in Section 2.1.2). Each floor design option should be subsequently tested for their structural performance via numerical analysis, which is part of the future work beyond the scope of this study.

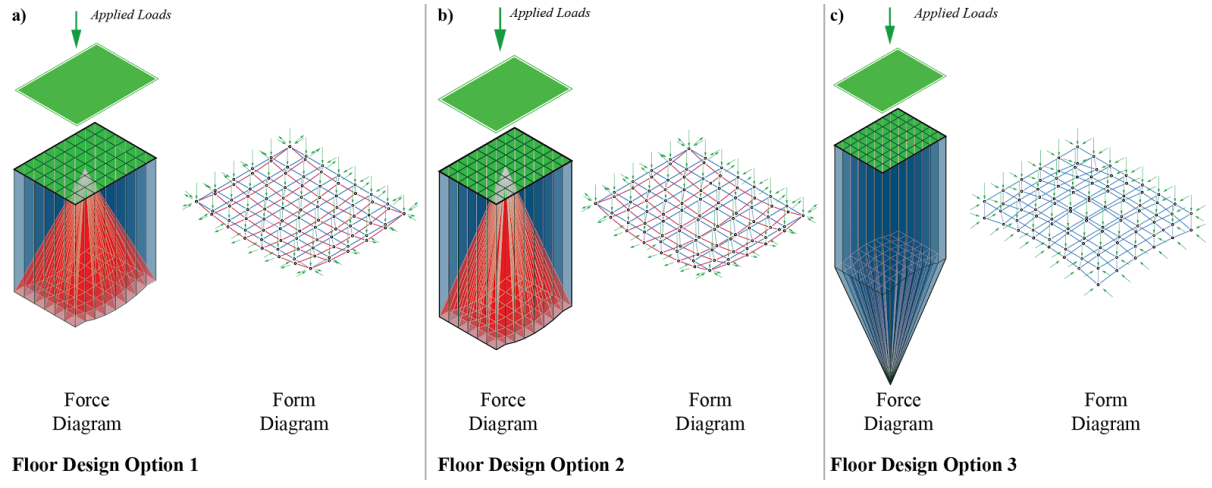

Figure 1: Form and force reciprocal diagrams for the design of funicular floor element options.

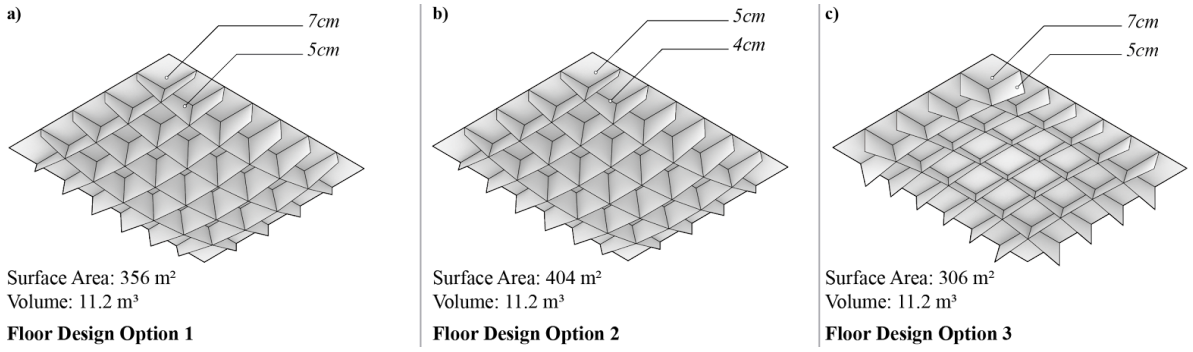

Figure 2: Funicular floor element design options derived from the form and force diagrams. Surface area, concrete topping and rib thickness, and material volumes are tracked for each option.

2.1.2. Thermal mass performance

The versatility of the structural form-finding process afforded by PGS allows us to generate different thermal mass distributions, and subsequently evaluate their thermal mass performance. Each floor design option materialized from the form-finding process has three constituent geometric parts, namely the flat floor slab atop, the internal oblique or vertical rib surfaces, and downward facing ceiling surfaces. For the three design options presented in this study, only the flat topping and internal ribs are materialized from the form diagram as faces for most surface area exposure.

We selected three funicular floor design options where each has different material thicknesses and exposed surface area (Figure 2), while constrained by the overall material volume equivalent to the flat concrete slab. These geometric parameters can provide different response time and thermal mass performance for cooling, which is then tested in the building energy model (detailed in Section 2.2). Table 1 presents the thermal and structural properties assumed for the concrete floor element.

Table 1: thermal and structural properties of the floor element designs.

	Conductivity [W/mK]	Density [kg/m3]	Specific heat [J/(kg K)]	Roughness	Compressive strength [MPa]
Concrete	2.31	2322	832	Medium Smooth	25

2.2. Building Energy Model

This section describes using form-finding design geometries as input for whole building energy simulation. It details a case study on a secondary school building and its operation, assessing thermal mass performance and operational energy expenditure for selected funicular floor design options.

2.2.1. Case study building

We reference the US Department of Energy (DoE) Secondary School Building as the baseline and simulated under the mixed-mode scenario where both natural ventilation and mechanical HVAC using Ideal Loads Air System work cooperatively. To compare different concrete funicular floor element design options on their impact on operational energy and subsequent carbon emission, we specifically focus our analysis on a pair of south facing corner classrooms for this study (Figure 3). The default floor construction of the corner classrooms has a flat, 0.1016 m thick, concrete floor slab topped by a carpet layer. The carpet layer is removed to expose concrete floor structure to maximize thermal mass surface exposure to air and performance. The flab floor slab thickness is adjusted to 0.1131 m to ensure the overall material volume of concrete is the same between the flat slab baseline and funicular floor design options.

The International Energy Conservation Code (IECC) U.S. climate 3C (marine in San Diego, California) and 5B (cold in Denver, Colorado) climate zones are selected as the outdoor climatic condition, both for its reported internal thermal mass (ITM) operational energy saving potential [11]

and varying degrees of grid electrification and associated carbon emission reduction timeline from 2020 to 2080. Future meteorological year (fTMY) EnergyPlus Weather files generated by the ACCESS-CM2 climate model projection [12], [13], [14] are used for building energy simulation to estimate the impact of climate scenarios on annual operational energy use and thermal mass performance. Three fTMY files are used for each climate zone, considering the changing weather patterns from 2020 to 2039, 2040 to 2059, and 2060 to 2079.

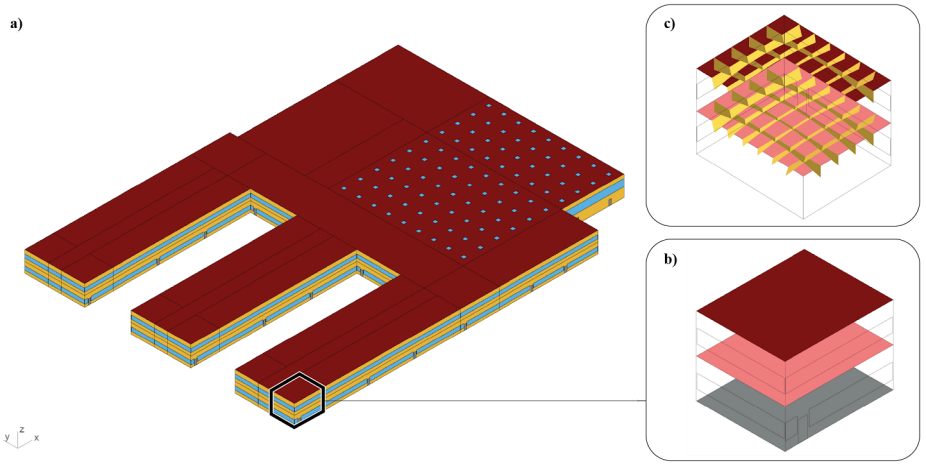

Figure 3: Building energy modeling geometry of a) the complete secondary school reference building, b) corner classrooms isolated as the focus of the performance analysis, and c) flipped view from below of the corner classrooms with funicular floor design. The concrete rib geometries generated from the form-finding process are highlighted in yellow.

2.2.2. Building energy model workflow

To seamlessly connect structural form-finding and building energy simulation workflows, we construct the building energy model (BEM) geometry in Rhinoceros, and use use Ladybug Tools (LBT) for Grasshopper to interface floor geometries designed with Polyframe and BEM simulated with OpenStudio and EnergyPlus. In this way, the parametrically designed floor geometries can have construction sets, programs, and additional energy modeling parameters directly assigned in the same form-finding modeling environment.

For each funicular floor design option, the flat topping surface is modeled as a Zone Surface, and the ribs surfaces are used as the geometric input of the Internal Mass object. The material thickness of each surface is assigned based on the values derived from the form-finding process.

2.2.3. Mixed-mode control strategies

Mixed-mode buildings employ a combination of natural ventilation and mechanical heating and cooling for space conditioning. Under the mixed-mode scenario, the mechanical heating and cooling system set points are widened to 20°C and 28°C to afford ITM and natural ventilation opportunities to mitigate heating and cooling loads. Natural ventilation is applied to maximize ITM performance potential and is simulated through the EnergyPlus Airflow Network. The windows of the corner classrooms are operable with 50% of its surface area consistent with a typical horizontally sliding window. The window discharge coefficient is at 0.45 for unobstructed aperture with insect screen. Cross ventilation is assumed for the classrooms with window openings facing two cardinal directions. Using an Energy Management System (EMS) program, the windows operation is dynamically controlled with a rule-based logic based on the desired minimum outdoor, and minimum and maximum indoor temperatures. 960 temperature combinations are tested on a 1°C increment using cooling carbon emission as the optimization objective. This workflow is applied for both studied climate zones, arriving at optimal maximum outdoor, and minimum and maximum indoor temperatures at 28°C, 23°C, and 28.5°C respectively for San Diego and Denver.

2.3. Life Cycle Operational Carbon Assessment

Greenhouse gas emissions associated with operational energy use for space cooling (Life Cycle Module B6) accumulate over the life of a building. In an all-electric building, these depend on electricity demand and the fuel sources supplying grid electricity, which vary throughout the day and year but also over longer time horizons in response to climate change, economics, and policy. This implies that static climate files and present-day grid emission factors may be inadequate for supporting long-term projections. Our methodology supplants the use of retrospective weather files (TMY3, TMYx) with future weather files (fTMY) recently made available through Argonne National Laboratory [12], [13], [14].For each representative site in our study, we run whole building energy simulations using each of the four time periods available in the fTMY datasets (2020-39, 2040-59, and 2060-79). This allows us to predict hourly electricity demand for a full year within each time period. For future electricity grid emission factors, we utilize month-hour projections for corresponding balancing areas from the National Renewable Energy Lab's Cambium Mid-Case dataset [15]. The point-in-time product of hourly electricity demand (kWh) and grid emission factor ($kgCO_2e/kWh$) represents hourly operational emissions ($kgCO_2e$), which are then integrated over the full year to produce annual results. In this manner we account for the potential covariance between energy demand and grid emission factors, which is particularly significant in regions with a high proportion of renewable energy production. An added complication is the different temporal bounds and resolution in the fTMY and Cambium datasets: fTMY data cover in 20-year increments the full lifespan of a 60-year building, while Cambium data cover every two years until 2030, every 5 years from 2030 to 2050, and nothing beyond 2050. To address this misalignment, we apply the average annual geometric change in the Cambium data from 2030 to 2050 to extrapolate grid emission factors beyond 2050. Conversely, we apply geometric interpolation to the energy outputs from each 20-year fTMY time period as if it represented the mid-year in that range. In this manner 2050 is understood to be wholly represented by the output from the 2040-59 dataset, while 2060 is treated as the geometric average of the energy outputs from the 2040-59 and 2060-79 datasets.

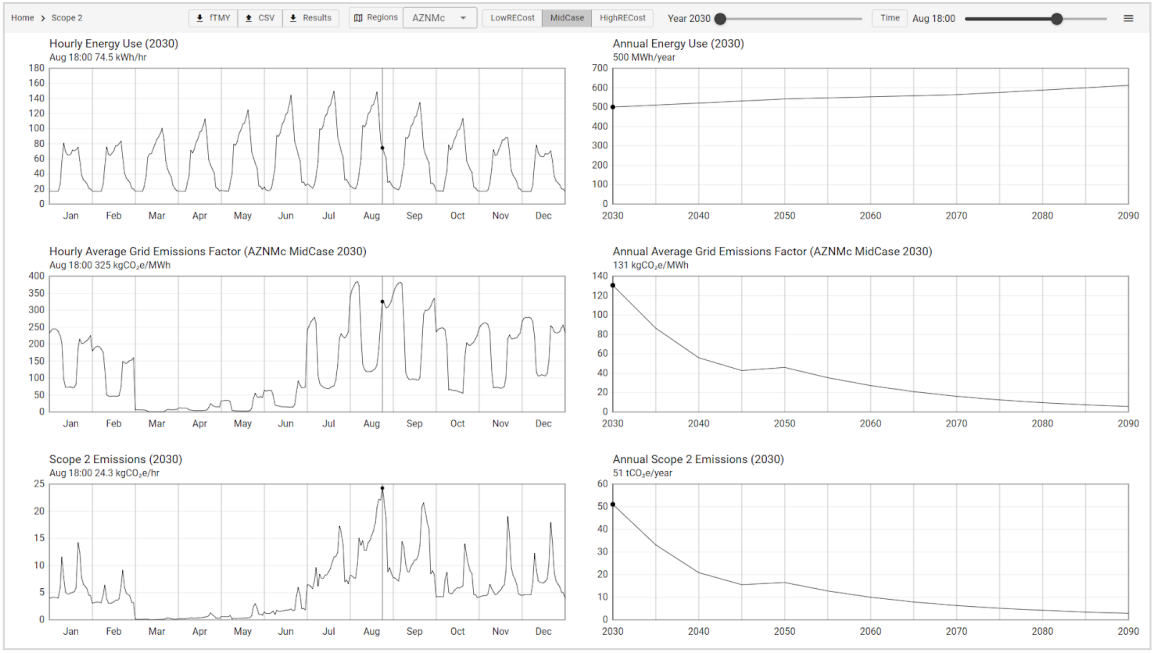

Figure 4: Interface for visualizing operational emission data as the product of energy use and grid emissions.

Figure 4 illustrates the entirety of the operational emissions methodology and underscores the importance of considering hourly, seasonal, and long-term variations in both energy use and grid emission factors. The left side of Figure 4 illustrates hourly variations in energy use (top), emission factors (middle), and their product (bottom) for the year 2030 using an energy model simulation of a reference building, based on the Tucson, Arizona 2020-2039 ACCESS-CM2 fTMY file and AZMNc

Cambium emission assessment region. The highlighted month-hour of August 18:00 corresponds to the maximum hourly emissions value for that year of 24.3 $kgCO_2e/hr$. Notably, this does not correspond to the hourly peak in either energy use or in emission factor, individually - only to their product. Also noteworthy are the negligible emissions from March through May due to the near-zero emission factors during this period. The right side of Figure 4 shows cumulative annual energy use (top), average annual grid emission factor (middle), and cumulative annual emissions (bottom) over a 60-year building life, where the selected 2030 year in each graph derives from the corresponding graph to its immediate left. Note that the lower figure of 51 tCO_2e/yr is 28% less than the product of the upper two (500 MWh/yr x 131 $kgCO_2e/MWh$ = 65.5 tCO_2e/yr). This difference illustrates the importance of considering month-hourly covariance of energy and emission factors in favor of combining annual-average values. The downward trend in annual operational emissions observed in the lower graph highlights the dominance of grid decarbonization over modest increases in annual energy use due to climate change. In locations where the energy grid is predicted to decarbonize rapidly, we would expect to see similar patterns.

3. Life Cycle Cooling Carbon Emission Results

Across three design options, we observe a net positive cooling carbon emission reduction across most studied climate zones and a large portion of the building life cycles. In San Diego, all design options exhibit cooling carbon emission reduction compared to the flat slab from 2020 to 2039, particularly during the morning and early afternoon period. As the cooling demand increases from 2040 to 2059 due to climate change, the thermal mass performance of all the concrete floor design options reach their diminishing return earlier during the course of a day. Therefore, the net cooling carbon emission reduction benefits are moderately reduced, particularly in the afternoon hours. However, October now enjoys an increase in emission reduction benefit compared to the 2020 to 2039 period. From 2060 to 2079, given California's 100% electricity grid decarbonization goal, the grid emission factors are 0 in all hours. Nonetheless, all design options can reduce cooling energy use and provide indoor temperature damping and shift benefits in reducing cooling demand. The net cooling energy use reduction and cooling carbon emission reduction for each funicular floor design options compared to the flat concrete slab baseline are tabulated as percentage in Table 2. Figure 5 illustrates the month-hour carbon emission associated with space cooling with temporal resolution.

In Denver, using concrete funicular floor with expanded surface area exposure also proves to be advantageous to reducing cooling carbon emission compared to the flat slab due to enhanced thermal mass performance (Table 4). From 2020 to 2039, all design options show reduction potential during the morning hours with the benefit peaking at the early afternoon hours (Figure 6). In the late afternoon, a negative reduction in cooling carbon emission is observed across all design options, signaling the thermal mass can no longer reduce cooling load. Depending on the surface area exposure, thickness, and material distribution of the funicular floor design, the carbon emission associated with cooling can be delayed. For example, design option 1 shows the largest peak emission reduction and the ability to maintain the net emission reduction benefit the longest. This augmented performance may be attributed to the most surface area exposed for optimal conduction and substantial thickness for thermal storage. With increased cooling demand from 2040 to 2059, the overall emission reduction benefit decreases by 5% for design option 1 and 2. With the least surface area exposed, design option 3 can no longer provide cooling carbon emission reduction benefit, and continues to show diminishing performance from 2060 to 2079.

Table 2: Annual cooling energy use (CEU) and cooling carbon emission (CCE) reduction percentages from the flat slab baseline for each design option in San Diego, California from 2020 to 2079.

	Design Option 1		Design Option 2		Design Option 3	
	CEU	CCE	CEU	CCE	CEU	CCE
2020 - 2039	-26.6%	-24.8%	-14.2%	-11.0%	-14.1%	-12.7%
2040 - 2059	-13.6%	-8.7%	-9.5%	-3.6%	-2.4%	1.9%
2060 - 2079	-14.1%	0%	-9.8%	0%	-2.6%	0%

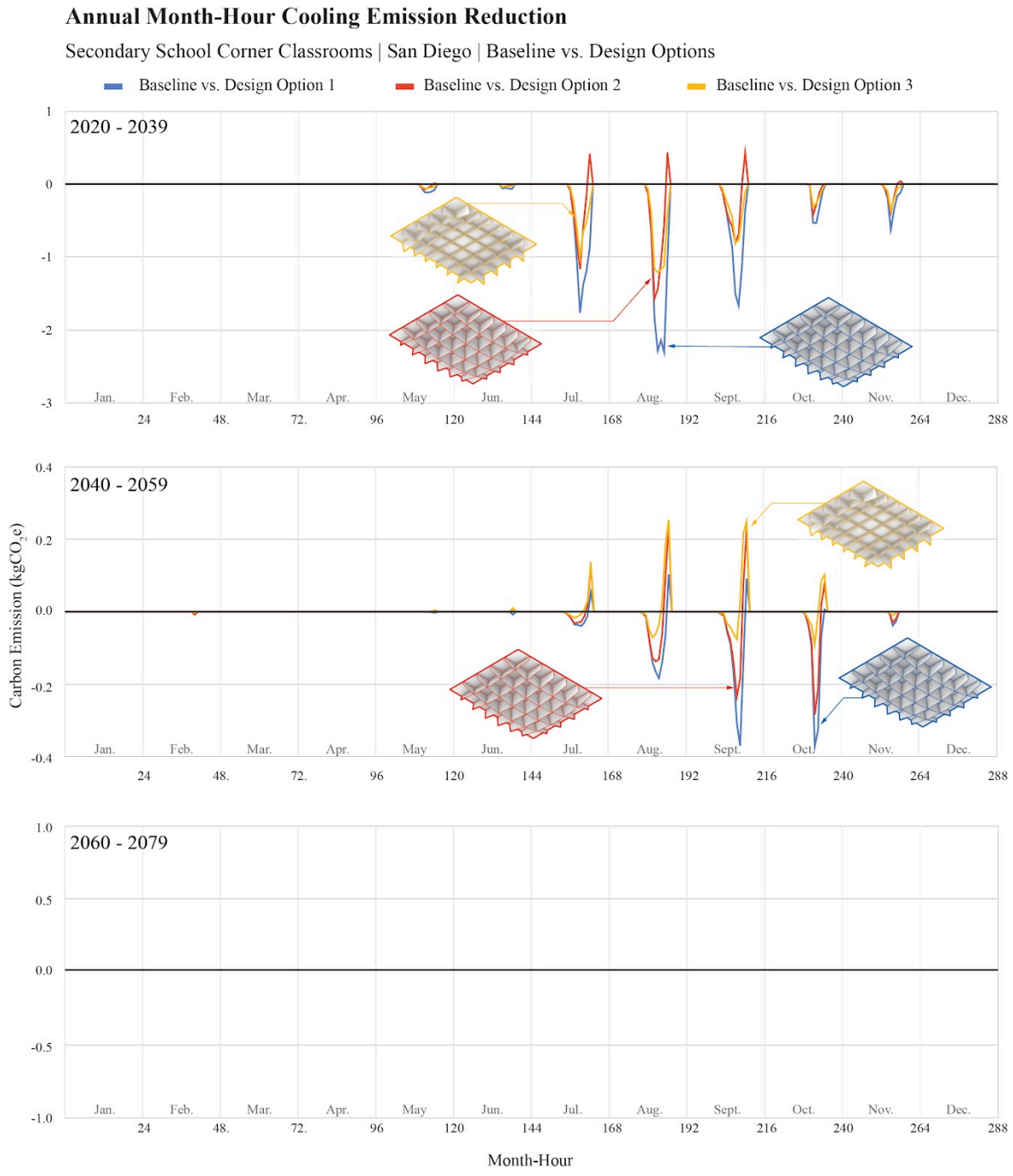

Figure 5: Annually hourly operational carbon emission improvement for 3 floor design options from the flat concrete slab baseline from a) 2020 to 2039, b) 2040 to 2059, and c) 2060 to 2079 in San Diego, California.

Table 3: Annual cooling energy use (CEU) and cooling carbon emission (CCE) reduction percentages from the flat slab baseline for each design option in Denver, Colorado from 2020 to 2079.

	Design Option 1		Design Option 2		Design Option 3	
	CEU	CCE	CEU	CCE	CEU	CCE
2020 - 2039	-16.2%	-15.3%	-10.3%	-9.3%	-1.4%	-0.7%
2040 - 2059	-14.9%	-10.0%	-9.3%	-4.3%	-1.4%	2.0%
2060 - 2079	-12.2%	-6.1%	-7.1%	-0.2%	-0.6%	-4.3%

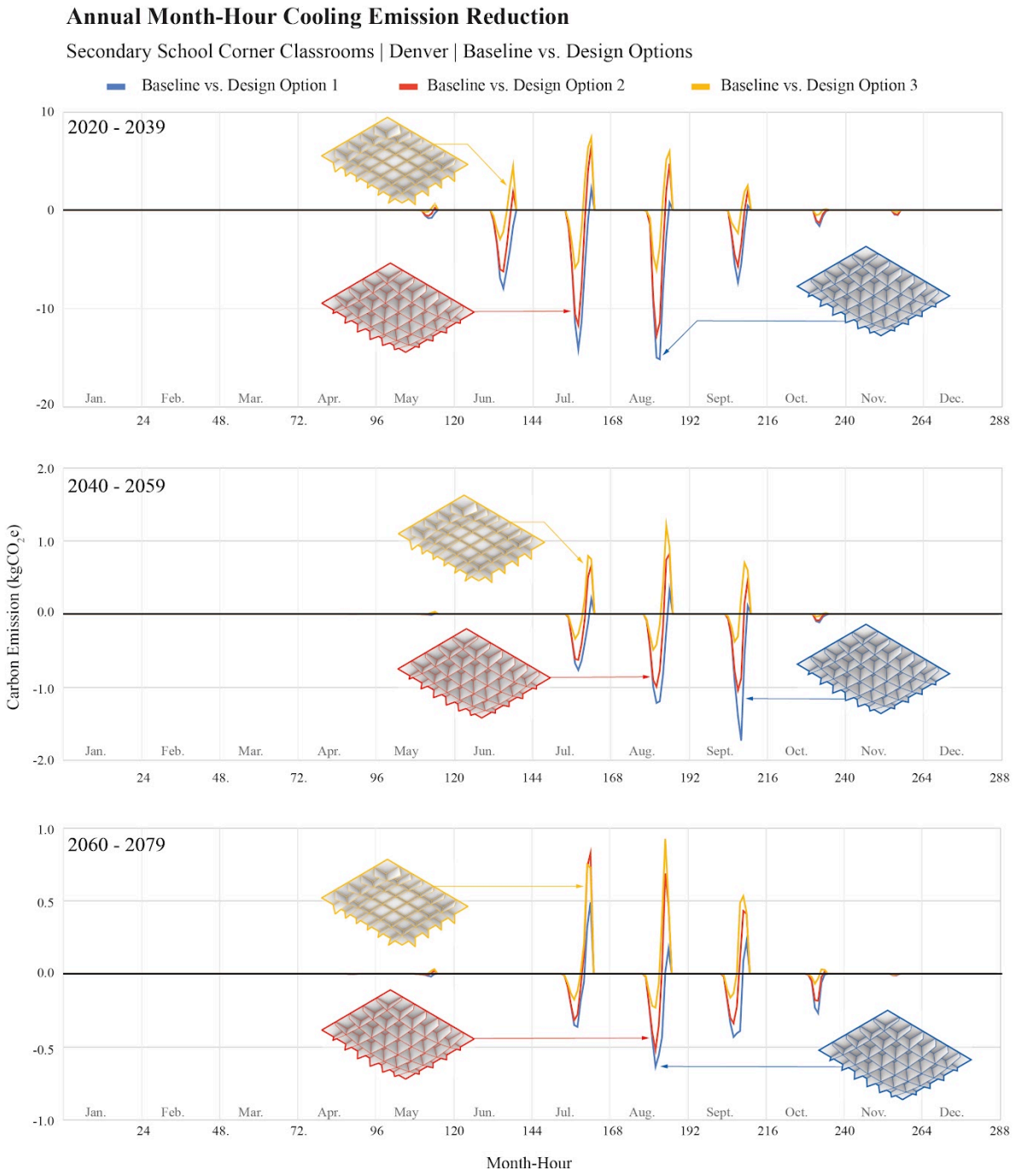

Figure 6: Annually hourly operational carbon emission improvement for 3 floor design options from the flat concrete slab baseline from a) 2020 to 2039, b) 2040 to 2059, and c) 2060 to 2079 in Denver, Colorado.

4. Conclusion

We present a parametric co-design workflow that considers structurally optimized funicular floors and their associated thermal mass performance in the early design process. Specifically, we leverage the robust form-finding versatility of PGS in designing funicular forms for expanded surface area exposure and constraining material volume, and connect that with building energy simulation. Taking advantage of their ability to act as a thermal battery to reduce operational energy consumption for mechanical cooling, we assess the operational carbon emission of each funicular concrete floor design option in two climate zones and grid emission scenarios for their projected 60 year building use.

Our results reveal that using structurally optimized funicular floor elements as BTM can better reduce and shift diurnal and seasonal cooling energy expenditure compared to the conventional flat concrete slab of the same material volume. This performance improvement induced by geometry provides corresponding buffer and reduction on daily grid emission during the morning peak ramp and peak energy consumption period where renewable energy sources such as solar may be under-capacity. In addition, we see a carbon emission reduction associated with the BTM performance during the shoulder seasons where natural ventilation reduces the reliance on mechanical cooling. With the best design option, a 25% and 15% annual cooling carbon emission reduction can be achieved in San Diego and Denver from 2020 to 2039. As the electricity grid transitions to low emission sources, there is still a 9% and 10% reduction from 2040 to 2059. From 2060 onwards, the best design option continues to provide operational cooling energy reduction, despite the diminishing cooling carbon emission reduction benefit due to the 100% grid decarbonisation goals. Therefore, these findings suggest the importance of optimally tuning the surface exposure, thickness and overall material distribution of the concrete funicular floor elements during the early stage form-finding process.

Consequently, our integrated workflow demonstrates potential in carbon emission reduction for the simultaneous consideration of funicular floor design and thermal mass performance in the early design stage. This work opens up thermal mass performance consideration and augmentation as part of the structural form-finding process using PGS – a direction that warrants further future research.

Acknowledgements

The authors acknowledge the support provided by the Advanced Research Projects Agency–Energy (ARPA-E) Grant of the U.S. Department of Energy (DE-AR0001631) to Dr. Masoud Akbarzadeh and Dr. Dorit Aviv.

References

[1] International Energy Agency, Global Alliance for Buildings and Construction, the United Nations, and United Nation Environment Programme, “2019 Global Status Report for Buildings and Construction: Towards a Zero-Emission, Efficient and Resilient Buildings and Construction Sector,” United Nation Environment Programme, Global, Governmental Report, 2019. Accessed: Nov. 30, 2023. [Online].

[2] United Nation Environment Programme, “Global Cooling Watch 2023: Keeping it Chill: How to meet cooling demands while cutting emissions,” United Nation Environment Programme, Nairobi, 2023. Accessed: Apr. 16, 2024. [Online]. Available: doi.org/10.59117/20.500.11822/44243

[3] S. Verbeke and A. Audenaert, “Thermal inertia in buildings: A review of impacts across climate and building use,” *Renew. Sustain. Energy Rev.*, vol. 82, pp. 2300–2318, Feb. 2018.

[4] S. Craig, “The optimal tuning, within carbon limits, of thermal mass in naturally ventilated buildings,” *Build. Environ.*, vol. 165, p. 106373, Nov. 2019.

[5] J. N. Hacker, T. P. De Saulles, A. J. Minson, and M. J. Holmes, “Embodied and operational carbon dioxide emissions from housing: A case study on the effects of thermal mass and climate change,” *Energy Build.*, vol. 40, no. 3, pp. 375–384, Jan. 2008.

[6] C. R. Iddon and S. K. Firth, “Embodied and operational energy for new-build housing: A case study of construction methods in the UK,” *Energy Build.*, vol. 67, pp. 479–488, Dec. 2013.

[7] M. Akbarzadeh *et al.*, “Diamanti: 3D-Printed, Post-tensioned Concrete Canopy,” in *FABRICATE 2024: Creating Resourceful Futures*, Copenhagen: UCL Press, 2024.

[8] Z. Wang, X. Zhang, X. Peng, S. Vasanthakumar, and D. Aviv, “Augmenting Thermal Mass Performance without Added Carbon Footprint: Surface Area Modulation of Structural Slabs in Naturally Ventilated Buildings,” in *Proceedings of IBPSA-USA SimBuild 2024 Conference*, Denver, Colorado: International Building Performance Simulation Association, May 2024.

[9] A. Nejur and M. Akbarzadeh, “PolyFrame, Efficient Computation for 3D Graphic Statics,” *Comput.-Aided Des.*, vol. 134, May 2021.

[10] M. Hablicsek, M. Akbarzadeh, and Y. Guo, “Algebraic 3D graphic statics: Reciprocal constructions,” *Comput.-Aided Des.*, vol. 108, pp. 30–41, Mar. 2019.

[11] A. Reilly and O. Kinnane, “The impact of thermal mass on building energy consumption,” *Appl.*

Energy, vol. 198, pp. 108–121, Jul. 2017.
[12] B. Bass, J. New, D. Rastogi, and S.-C. Kao, "Future Typical Meteorological Year (fTMY) US Weather Files for Building Simulation." Zenodo, Jul. 29, 2022.
[13] S. Chowdhury, F. Li, A. Stubbings, J. New, D. Rastogi, and S.-C. Kao, "Future Typical Meteorological Year (fTMY) US Weather Files for Building Simulation for every US County (East and South)." Zenodo, Sep. 11, 2023.
[14] S. Chowdhury, F. Li, A. Stubbings, J. New, D. Rastogi, and S.-C. Kao, "Future Typical Meteorological Year (fTMY) US Weather Files for Building Simulation for every US County (West and Midwest)." Zenodo, Sep. 11, 2023.
[15] P. Gagnon *et al.*, "Cambium 2022 Data," National Renewable Energy Laboratory. Accessed: Apr. 15, 2024. [Online].